

Numerical simulation of Bell inequality's violation using optical transverse modes in multimode waveguides

Jian Fu, and Xun Zhang

*State Key Lab of Modern Optical Instrumentation,
Centre for Optical and Electromagnetic Research,
Department of Optical Engineering,
Zhejiang University, Hangzhou 310027, China*

Abstract

We numerically demonstrate that “mode-entangled states” based on the transverse modes of classical optical fields in multimode waveguides violate Bell's inequality. Numerically simulating the correlation measurement scheme of Bell's inequality, we obtain the normalized correlation functions of the intensity fluctuations for the two entangled classical fields. By using the correlation functions, the maximum violations of Bell's inequality are obtained. This implies that the two classical fields in the mode-entangled states, although spatially separated, present a nonlocal correlation.

PACS numbers: 03.67.Mn, 42.50.-p

Quantum entanglement is a fundamental concept and one of the most interesting properties of quantum mechanics. The importance of quantum entanglement in quantum information processing is by now widely appreciated [1, 2, 3]. Quantum entanglement is first introduced by Einstein, Podolsky, and Rosen (EPR) as most noticeable the EPR paradox [4], which is at the origin of quantum nonlocality. Bell proposed a remarkable inequality imposed by a local hidden variable theory, which enables an experimental test on the quantum nonlocality [5]. The violation of Bell’s inequality indicates the presence of quantum entanglement. Generally, the nonlocal properties, which appear in the correlation measurement of quantum entangled states for two spatially separated particles, are considered as the inherent features of quantum theory with no classical analog. Numerous theoretical studies and experimental demonstrations have been carried out to understand the nonlocal properties of quantum states. It is noticeable that the violation of Bell’s inequality is possible in nonlinear optical processes such as multimode parametric amplifiers and four-wave mixing, in which the output modes are in some way correlated [6]. In order to explore the intrinsic quantum entanglement, some researchers yet use classical optical fields to simulate quantum entanglement numerically and experimentally [7, 8].

The similarities between the Helmholtz equation and the Schrödinger equation have attracted some researches on the analogies between the transverse modes in multimode waveguides and the quantum Fock states [9, 10, 11]. Besides the uncertainty relation [12], Wigner phase-space distributions of the optical multimode fields exhibiting negative regions are similar to quantum Fock states, which had been verified experimentally [13, 14]. Farther, some researchers have argued convincingly that the classical Maxwell field plays the role of the quantum wave function for a single photon [15]. This might be the physical basis of the similarities. However, the similarities have been limited principally to the measurement of first-order coherence, i.e., single-particle states. Classical wave analogs of the high-order nonlocal coherence (quantum entanglement), i.e., multiparticle states, have been seldom studied [7]. The researches on the high-order local coherence can date back to the theoretical and experimental researches on interferences of two independent laser beams in Refs. [16, 17]. Due to the random phase difference between the two beams, no stable but transient interference fringes can be observed. These local effects can be well explained by quantum theory and classical electromagnetics. Recently, “mode-entangled states” based on the transverse modes of classical optical fields propagating in multimode waveguides are proposed as the classical

simulation of quantum entangled states [18]. The states can be regarded as the nonlocal generalization of the high-order local coherence. It is interesting that the mode-entangled states can also show the nonlocal correlations such as the violation of Bell’s inequality and the nonlocal properties of optical pulses’ group delays. However, the nonlocal correlations are generally considered as the inherent features of quantum entanglement.

In this letter, we numerically demonstrate that the mode-entangled states violate Bell’s inequality by completely using classical electromagnetics. Numerically simulating the correlation measurement scheme proposed in Ref. [18], we obtain the normalized correlation functions of the intensity fluctuations for two entangled classical fields. Then the correlation functions are substituted into Bell’s inequality and the maximum violations of Bell’s inequality are obtained. Despite all that, the mode-entangled states and the quantum entangled states, from a physical viewpoint, are different because the measurements of classical fields and quantum states are different. The research on this simulation may be important, for it not only helps to understand the nonlocal properties of quantum entanglement from a new viewpoint, but also arouses interest in a full optical quantum computation scheme based on the transverse modes of classical fields [19, 20]. And besides, it may be attractive to other research fields. Such as researches on matter waves of Bose-Einstein condensates, similar to the scheme, a quantum computation scheme based on the transverse modes of the guided matter waves [21] is also interesting.

In the correlation measurement scheme of Bell’s inequality proposed in Ref. [18], two independent monochromatic classical fields are prepared to input a CNOT gate as the control and the target fields, respectively. When the control field is given at mode superposition states $(|TE_0\rangle \pm |TE_1\rangle)/\sqrt{2}$ and the target field is given at the mode $|TE_0\rangle$ or $|TE_1\rangle$, the output states of the CNOT gate are so called “mode-entangled states”,

$$\begin{aligned} |\Phi_1^\pm\rangle &= \frac{1}{\sqrt{2}} (|TE_0\rangle_c |TE_0\rangle_t \pm |TE_1\rangle_c |TE_1\rangle_t), \\ |\Psi_1^\pm\rangle &= \frac{1}{\sqrt{2}} (|TE_0\rangle_c |TE_1\rangle_t \pm |TE_1\rangle_c |TE_0\rangle_t), \end{aligned} \quad (1)$$

where subscripts c and t represent the control and the target fields, respectively. The states in each waveguide are mode superpositions, which are obviously different from product

states,

$$\begin{aligned} |\Psi_2\rangle &= |\Psi_c\rangle \otimes |\Psi_t\rangle \\ &= \frac{1}{2} (|\text{TE}_0\rangle_c \pm |\text{TE}_1\rangle_c) (|\text{TE}_0\rangle_t \pm |\text{TE}_1\rangle_t), \end{aligned} \quad (2)$$

where $|\Psi_c\rangle$ and $|\Psi_t\rangle$ represent the states of control and target fields, respectively. The difference can be obtained not by measuring the single field, but by the correlation measurement of the control and the target fields. The correlation measurement can present that the two entangled fields are inseparable to some extent, which is a nonlocal correlation.

To perform the correlation measurement of Bell's inequality, the control and the target fields output from the CNOT gate are sent to spatially separated (independent) mode analyzers (MAs), each of which contains a Y splitter and a variable phase modulator θ_1 (θ_2). Based on the correlation analysis, we get the correlation function,

$$S(\theta_1, \theta_2) = \left\langle \hat{A}_c(\theta_1) \hat{B}_t(\theta_2) \right\rangle, \quad (3)$$

where $\hat{A}_c(\theta_1)$ and $\hat{B}_t(\theta_2)$ are the intensity difference operators of the MAs' outputs for the control and target fields, respectively,

$$\begin{aligned} \hat{A}_c(\theta_1) &= \hat{I}_c^+(\theta_1) - \hat{I}_c^-(\theta_1) \\ &= e^{2i\theta_1} |\text{TE}_0\rangle_c \langle \text{TE}_1|_c + e^{-2i\theta_1} |\text{TE}_1\rangle_c \langle \text{TE}_0|_c, \\ \hat{B}_t(\theta_2) &= \hat{I}_t^+(\theta_2) - \hat{I}_t^-(\theta_2) \\ &= e^{2i\theta_2} |\text{TE}_0\rangle_t \langle \text{TE}_1|_t + e^{-2i\theta_2} |\text{TE}_1\rangle_t \langle \text{TE}_0|_t, \end{aligned} \quad (4)$$

with $\hat{I}_c^\pm(\theta_1)$ and $\hat{I}_t^\pm(\theta_2)$ being the MA's operations on the control and the target fields, respectively. Apparently, there is no correlation between the independent measurements of the two fields in the product states, hence, their correlation function can be written as the product of the expected values,

$$\begin{aligned} S_{\Psi_2}(\theta_1, \theta_2) &= \langle \Psi_2 | \hat{A}_c(\theta_1) \hat{B}_t(\theta_2) | \Psi_2 \rangle \\ &= \langle \Psi_c | \hat{A}_c(\theta_1) | \Psi_c \rangle \cdot \langle \Psi_t | \hat{B}_t(\theta_2) | \Psi_t \rangle. \end{aligned} \quad (5)$$

However, the correlation function of the mode-entangled states can not be written in such form because the results of the independent measurements of the two entangled fields are correlated. Here Bell's inequality is given as the criterion to distinguish the mode-entangled state and the product state.

Consider an ensemble (large collection) of the independent and identical systems that are labeled by λ that satisfies normalization condition $\int_{\Lambda} \rho(\lambda) d\lambda = 1$, where $\rho(\lambda)$ is a distribution function and Λ is spanned by λ . In this model, the correlation function can be rewritten as a normalized form

$$\begin{aligned} S(\theta_1, \theta_2) &= \langle A_c(\theta_1) B_t(\theta_2) \rangle \\ &= \int_{\Lambda} A'_c(\theta_1, \lambda) B'_t(\theta_2, \lambda) \rho(\lambda) d\lambda, \end{aligned} \quad (6)$$

with

$$\begin{aligned} A'_c(\theta_1, \lambda) &= \frac{A_c(\theta_1, \lambda)}{[\int_{\Lambda} A_c^2(\theta_1, \lambda) \rho(\lambda) d\lambda]^{1/2}}, \\ B'_t(\theta_2, \lambda) &= \frac{B_t(\theta_2, \lambda)}{[\int_{\Lambda} B_t^2(\theta_2, \lambda) \rho(\lambda) d\lambda]^{1/2}}, \end{aligned} \quad (7)$$

where $A_c(\theta_1, \lambda)$ and $B_t(\theta_2, \lambda)$ are the correlation measurement results corresponding to each λ . Using the property of the product state's correlation function shown in Eq. (5), Schwarz inequality $|S(\theta_1, \theta_2)| \leq 1$ and Eq. (6), we obtain

$$\begin{aligned} |S(\theta_1, \theta_2) - S(\theta_1, \theta'_2)| &\leq 1 \pm \int_{\Lambda} A'_c(\theta'_1, \lambda) B'_t(\theta'_2, \lambda) \rho(\lambda) d\lambda \\ &\quad + \left[1 \pm \int_{\Lambda} A'_c(\theta'_1, \lambda) B'_t(\theta_2, \lambda) \rho(\lambda) d\lambda \right] \\ &= 2 \pm [S(\theta'_1, \theta'_2) + S(\theta'_1, \theta_2)], \end{aligned} \quad (8)$$

then Bell's inequality (CHSH inequality [22]) is given explicitly as

$$|B| = |S(\theta_1, \theta_2) - S(\theta_1, \theta'_2) + S(\theta'_1, \theta'_2) + S(\theta'_1, \theta_2)| \leq 2, \quad (9)$$

which implies that the violation of Bell's inequality never occurs for the product states. On the contrary, if the violation occurs, there is a nonlocal correlation between the two fields of the mode-entangled states. In Ref. [6], Bell's inequalities are generalized for the case of fields or arbitrary intensity and the violation of Bell's inequalities is shown to be possible in a regime showing strong violation of Schwarz inequality. But the Schwarz inequality, related to the phenomena of photon antibunching and squeezing, is different from $|S(\theta_1, \theta_2)| \leq 1$ satisfied by the correlation function.

Let us now numerically simulate the scheme shown in Fig. 1 to obtain the correlation functions of the control and the target fields. For such purpose, we have to simulate the two

independent optical fields propagating in waveguides. In Refs. [16, 17], the two independent light beams are replaced by two monochromatic optical fields with random phases φ_1 and φ_2 uniformly distributed in $[0, 2\pi]$. Therefore, the two independent optical fields propagating in the waveguides can be regarded as an ensemble labeled by the phase difference $\lambda = \varphi_1 - \varphi_2$, which also is a random variable uniformly distributed in $[0, 2\pi]$. Thus, a simulation of each λ is equivalent to an independent experiment of the ensemble, then the integrals of the simulations describe the behaviors of two independent optical fields. Although it requires infinite numbers of the simulations in theory, we can assign λ with discrete values in practice to realize the ergodicity of λ by finite numbers of the simulations.

The finite differential beam propagation method (FD-BPM) employed in our numerical simulation is widely used in the analysis of optical waveguides and well proved effective and reliable by a lot of researchers [23]. Utilizing FD-BPM, the evolution of waveguide modes are clearly demonstrated using intensity distributions. And the waveguide output intensities can be obtained by the integral of the intensity distributions. In the simulation of the scheme in Fig. 1, the two MAs are separated far enough to avoid disturbing each other, and the numerical simulation result is shown in Fig. 2. For a certain λ , we obtain the relation between the MAs' output intensities and θ_1 (θ_2) by changing the refractive indexes of the phase modulators. We find that the output intensities of MAs also change with the phase difference λ . The reason of the fact is that TE_0 modes of the control field and the target field in one of the Mach-Zehnder interferometer's arms, due to the phase difference λ , interfere with each other when they are passing through the directional couplers of the CNOT gate. The interference causes the intensity in Kerr-like medium varying with λ , therefore the phase shift via the Kerr effect also varies. Finally, the MAs' output intensities change with λ due to the phase shift. The intensity differences $A_c(\theta_1, \lambda)$ and $B_t(\theta_2, \lambda)$ versus θ_1 and θ_2 are shown in Fig. 3. While λ varies in $[0, 2\pi]$, $A_c(\theta_1, \lambda)$ and $B_t(\theta_2, \lambda)$ fluctuate around their mean values, and the ranges of the fluctuations change with θ_1 and θ_2 , respectively.

First, we obtain the random sequences $A_c(\theta_1, \lambda)$ and $B_t(\theta_2, \lambda)$ subjected to a sufficiently long random sequence of λ , then substitute them into Eq. (6), and obtain the correlation function $S(\theta_1, \theta_2)$ via summation of $A_c(\theta_1, \lambda)$ and $B_t(\theta_2, \lambda)$ instead of the integral of λ . The correlation functions $S(\theta_1, \theta_2)$ of $|\Phi_1^\pm\rangle$ and $|\Psi_1^\pm\rangle$ are shown in Fig. 4. After substituting $S(\theta_1, \theta_2)$ into Eq. (9), we obtain the maximum violation of Bell's inequality, as shown in Table 1, where the maximum values of $|B|$ are the average results of many λ 's sequences.

Considerable attention should be paid to that $S(\theta_1, \theta_2)$ shown in Fig. 4 are quite different from the correlation functions $\cos(2\theta_1 \pm 2\theta_2)$ or $\sin(2\theta_1 \pm 2\theta_2)$ of the quantum entangled states, therefore, θ_1 , θ'_1 , θ_2 and θ'_2 of the maximum violation of Bell's inequality in Table 1 may not be $\pi/8$, $-\pi/8$, 0 , and $\pi/4$. During the simulation, we find that the granularity of λ hardly influences the simulation results, so that the λ is assigned with 64 discrete values in $[0, 2\pi]$. Farther, we obtain the relation between the maximum of $|B|$ and the refractive index of the phase modulator θ_3 , as shown in Fig. 5.

In this letter, we have numerically demonstrated that the mode-entangled states generated by two independent classical fields propagating through the CNOT gate are different from the product states. The difference is presented in the correlation measurement of the two fields. For the mode-entangled states, Bell's inequality is violated. However, the violation never occurs for the product states. This implies that two classical fields in the mode-entangled states, although spatially separated, present a nonlocal correlation, which means the mode-entangled states can be really regarded as the classical simulation of quantum entangled states. The relevant experiments are necessary because they can prove the feasibility of our scheme, moreover, they might open new perspectives for optical quantum computation and communication.

This work was supported by the National Natural Science Foundation of China under Grant No. 60407003.

-
- [1] M. A. Nielsen and I. L. Chuang, *Quantum Computation and Quantum Information* (Cambridge University Press, Cambridge, 2000).
 - [2] C. H. Bennett, G. Brassard, and C. Crepeau et al., *Phys. Rev. Lett.* **70**, 1895 (1993).
 - [3] R. Jozsa and N. Linden, quant-ph/0201143; A. Ekert and R. Jozsa, *Philos. Trans. R. Soc. London* **356**, 1769 (1998); D. A. Lidar, *Appl. Phys. Lett.* **80**, 2419 (2002).
 - [4] A. Einstein, B. Podolsky, and N. Rosen, *Phys. Rev.* **47**, 777 (1935).
 - [5] J. S. Bell, *Physics* **1**, 195 (1964); J. S. Bell, *Speakable and Unsayable in Quantum Mechanics*, (Cambridge University Press, Cambridge, 1987).
 - [6] M. D. Reid and D. F. Walls, *Phys. Rev. A* **34**, 1260 (1986).
 - [7] K. F. Lee and J. E. Thomas, *Phys. Rev. Lett.* **88**, 097902 (2002).

- [8] W. A. Hofer, quant-ph/0108141; W. A. Hofer, quant-ph/0111131.
- [9] S. G. Krivoslykov, I. N. Sissakian, Opt. Quant. Elect. **12**, 463 (1980); S. G. Krivoslykov, *Quantum-Theoretical Formalism for Inhomogeneous Graded-Index Waveguides* (Akademie Verlag, Berlin, 1994).
- [10] G. Nienhuis and L. Allen, Phys. Rev. A **48**, 656 (1993).
- [11] D. Dragoman, Prog. Opt. **42**, 424 (2002); D. Dragoman, Optik **111**, 393 (2000); D. Dragoman, Optik **111**, 179 (2000).
- [12] D. Marcuse, *Light Transmission Optics* (Van Nostrand Reinhold, New York, 1972).
- [13] K. F. Lee, F. Reil, S. Bali, and A. Wax et al., Opt. Lett. **24**, 1370 (1999).
- [14] C. C. Cheng and M. G. Raymer, Phys. Rev. Lett. **82**, 4807 (1999).
- [15] J. E. Sipe, Phys. Rev. A **52**, 1875 (1995); I. Bialynicki-Birula, in *Progress in Optics XXXVI*, edited by E. Wolf, (Elsevier, Amsterdam, 1996); D. H. Kobe, Found. Phys **29**, 1203 (1999).
- [16] G. Magyar, and L. Mandel, Nature **198**, 255 (1963); L. Mandel, Phys. Rev. **134**, A10 (1964).
- [17] L. Mandel, J. Opt. Soc. Am. **52**, 1407 (1962).
- [18] J. Fu, Z. J. Si, and S. F. Tang et al., Phy. Rev. A **70**, 042313 (2004); quant-ph/0404095.
- [19] J. Fu, Proceedings of SPIE **5105**, 225 (2003); quant-ph/0211038.
- [20] M. A. Man'ko, V. I. Man'ko, and R. V. Mendes, Phys. Lett. A **288**, 132 (2001); R. Fedele and M. A. Man'ko, Eur. Phys. J. D **27**, 263 (2003).
- [21] E. Andersson, T. Calarco, and R. Folman et al., Phys. Rev. Lett. **88**, 100401 (2002).
- [22] J. F. Clauser, M. A. Horne, A. Shimony, and R. A. Holt, Phys. Rev. Lett. **23**, 880 (1969).
- [23] D. Yevick and B. Hermansson, IEEE J. Quantum Electron. **26**, 109 (1990); W. P. Huang, C. L. Xu, and S. T. Cu et al., J. Lightwave Technol. **10**, 295 (1992); G. Ronald Hadley, IEEE J. Quantum Electron. **28**, 363 (1992); R. Scarmozzino, A. Gopinath, and R. Pregla et al., IEEE J. Select. Topics Quantum Electron. **6**, 150 (2000); A. Locatelli, F. M. Pigozzo, and D. Modotto et al., IEEE J. Select. Topics Quantum. Electron. **8**, 440 (2002).

Fig. 1: Scheme of the numerical simulation.

Fig. 2: BPM simulation result for the scheme shown in Fig. 1 corresponding to $\lambda = 0$.

Fig. 3: The relation between the intensity differences and the phase modulators: (a) $A_c(\theta_1, \lambda)$ and θ_1 , (b) $B_t(\theta_2, \lambda)$ and θ_2 .

Fig. 4: The correlation functions $S(\theta_1, \theta_2)$ for mode-entangled states: (a) $|\Phi_1^+\rangle$, (b) $|\Phi_1^-\rangle$, (c) $|\Psi_1^+\rangle$, and (d) $|\Psi_1^-\rangle$.

Fig. 5: The maximum of $|B|$ versus the refractive index of the phase modulator θ_3 .

Tabel 1:

$ \Phi_1^+\rangle$	$\theta_1 = \frac{77}{40}\pi, \theta'_1 = \frac{35}{40}\pi, \theta_2 = \frac{73}{40}\pi, \theta'_2 = \frac{36}{40}\pi$	$\max B = 2.7834$
$ \Phi_1^-\rangle$	$\theta_1 = \frac{35}{40}\pi, \theta'_1 = \frac{38}{40}\pi, \theta_2 = \frac{111}{40}\pi, \theta'_2 = \frac{113}{40}\pi$	$\max B = 2.8041$
$ \Psi_1^+\rangle$	$\theta_1 = \frac{83}{40}\pi, \theta'_1 = \frac{75}{40}\pi, \theta_2 = \frac{112}{40}\pi, \theta'_2 = \frac{74}{40}\pi$	$\max B = 2.8084$
$ \Psi_1^-\rangle$	$\theta_1 = \frac{78}{40}\pi, \theta'_1 = \frac{35}{40}\pi, \theta_2 = \frac{72}{40}\pi, \theta'_2 = \frac{113}{40}\pi$	$\max B = 2.8086$

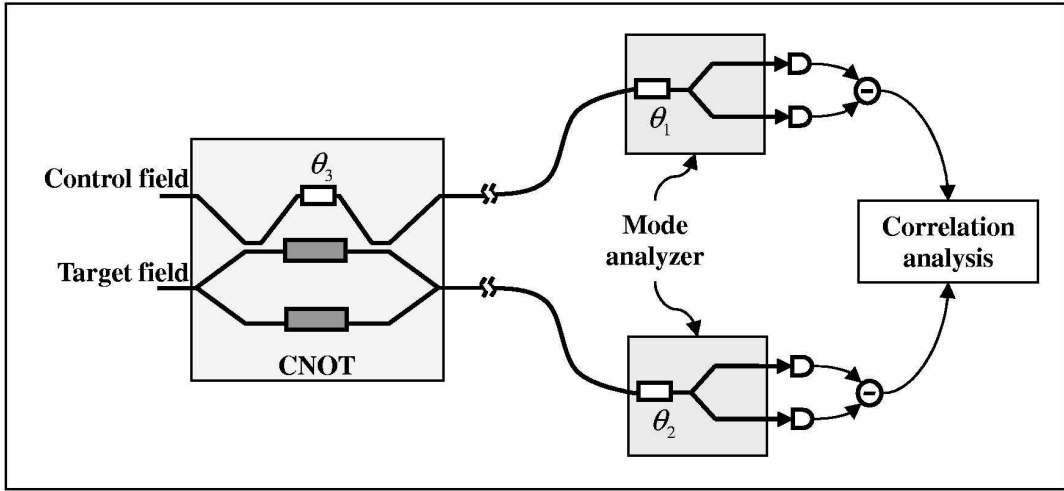


Fig. 1. Scheme of the numerical simulation.

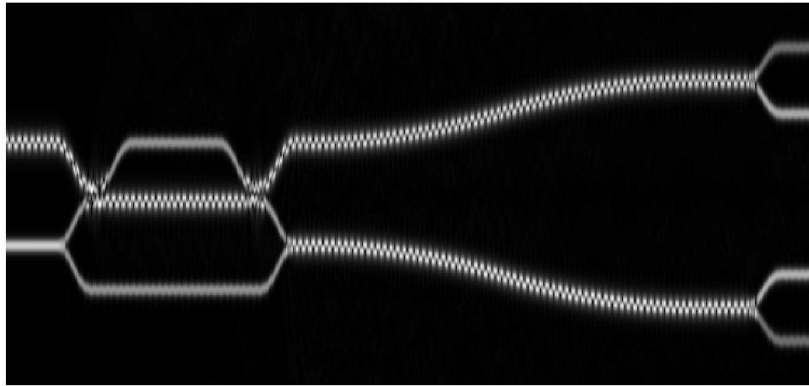


Fig. 2. BPM simulation result for the scheme shown in Fig. 1 corresponding to $\lambda = 0$.

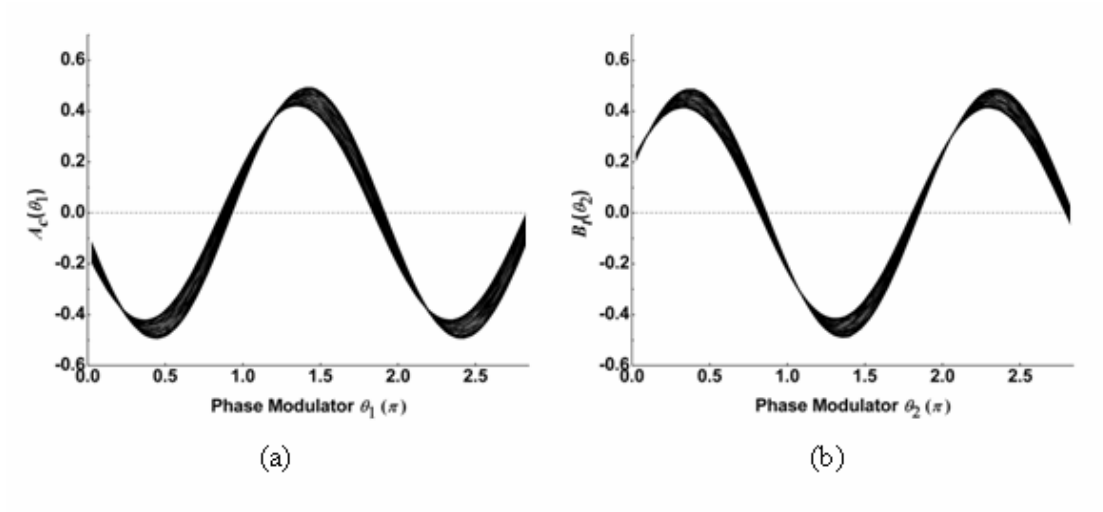


Fig. 3. The relation between the intensity differences and the phase modulators. (a) $A_c(\theta_1, \lambda)$ and θ_1 , (b) $B_r(\theta_2, \lambda)$ and θ_2 .

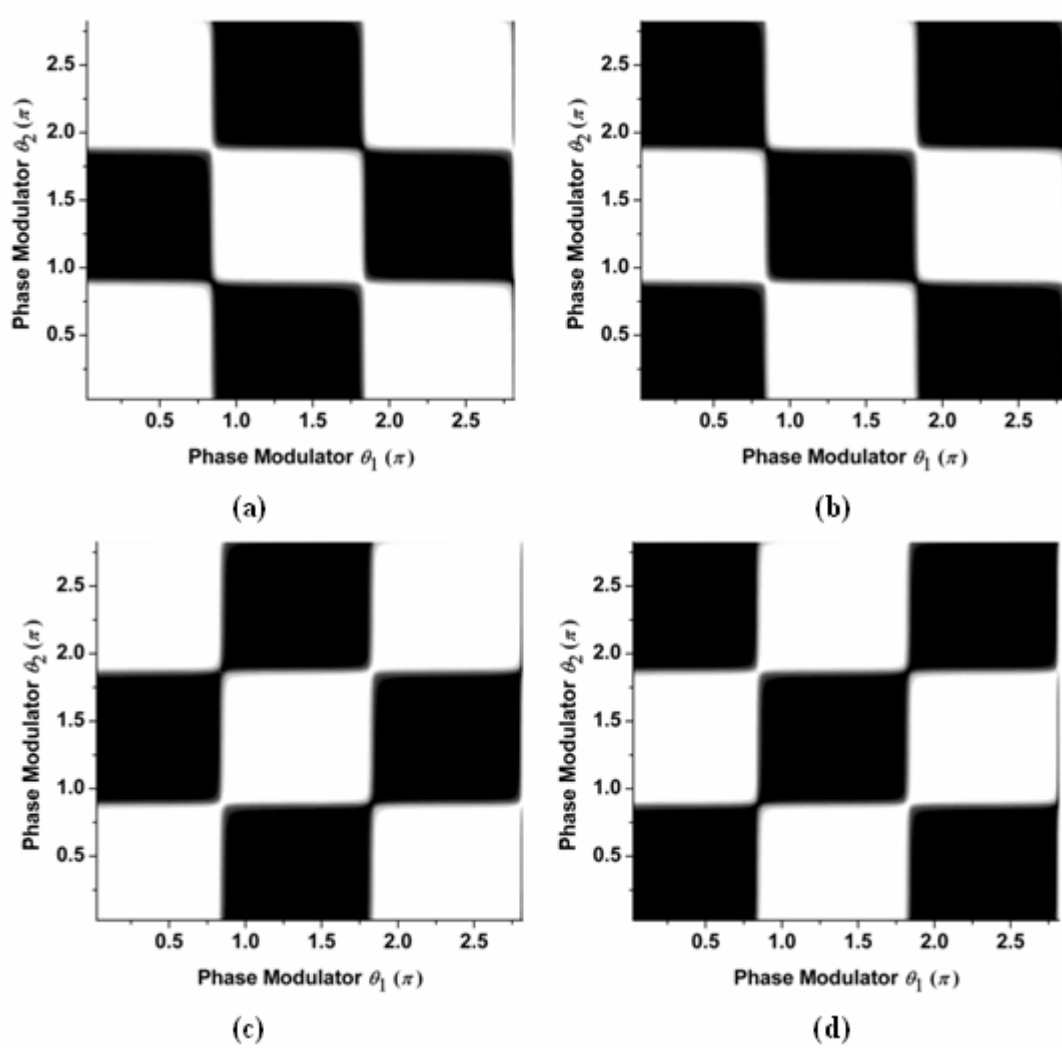


Fig. 4. The correlation functions $S(\theta_1, \theta_2)$ mode-entangled states: (a) $|\Phi_1^+\rangle$, (b) $|\Phi_1^-\rangle$, (c) $|\Psi_1^+\rangle$, and (d) $|\Psi_1^-\rangle$.

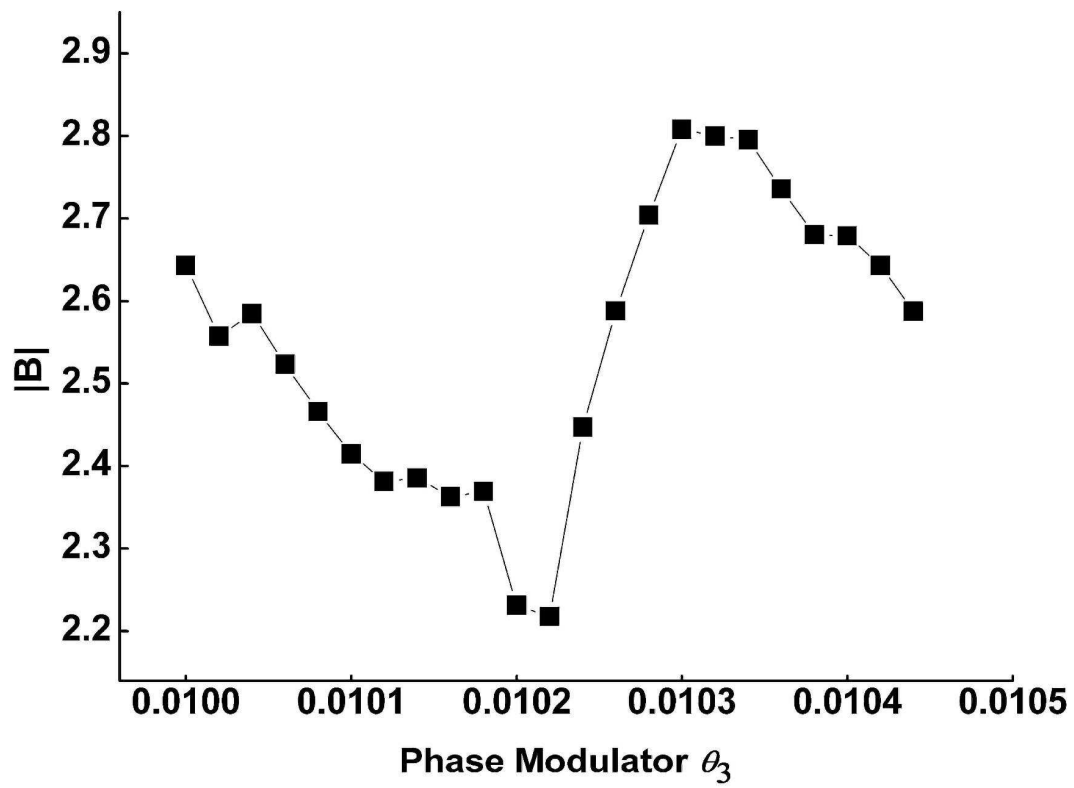


Fig. 5. $|B|$ versus the refractive index of the phase modulator θ_3